Available online at www.sciencedirect.com
ScienceDirect
Journal of the European Ceramic Society 31 (2011) 2005–2012
www.elsevier.com/locate/jeurceramsoc

Enhanced piezoelectric properties of $(Ba_{0.85}Ca_{0.15})(Ti_{0.9}Zr_{0.1})O_3$ lead-free ceramics by optimizing calcination and sintering temperature

Pan Wang, Yongxiang Li *, Yiqing Lu

The Key Lab of Inorganic Functional Materials and Device, Shanghai Institute of Ceramics, Chinese Academy of Sciences, 1295 Dingxi Road, Shanghai 200050, PR China

Received 8 January 2011; received in revised form 6 April 2011; accepted 17 April 2011
Available online 14 May 2011

Abstract

Lead-free $(Ba_{0.85}Ca_{0.15})(Ti_{0.9}Zr_{0.1})O_3$ (BCTZ) piezoelectric ceramics were prepared by conventional oxide-mixed method at various calcination and sintering temperatures. Both calcination and sintering temperatures have a significant effect on the density and grain size, which are closely related with piezoelectric and other properties of ceramics. The calcination temperature has a great influence on the grain boundary, which also plays an important role in piezoelectric properties. With increased calcination and sintering temperature, the ferroelectric and piezoelectric properties have enhanced significantly. The BCTZ ceramics calcined at 1300 °C and sintered at 1540 °C exhibit optimal electrical properties: $d_{33} = 650$ pC/N, $d_{31} = 74$ pC/N, $k_p = 0.53$, $k_t = 0.38$, $k_{31} = 0.309$, $s_{11}^E = 14.0 \times 10^{-12}$ m^2/N, $\varepsilon_r = 4500$, $P_r = 11.69$ μC/cm^2, which is a promising lead-free piezoelectric candidate.

Keywords: A. Calcination; A. Sintering; B. Grain boundaries; C. Piezoelectric properties

1. Introduction

The $Pb(Zr,Ti)O_3$ (PZT) based piezoelectric ceramics have dominated the commercial market of piezoelectric devices for more than half a century, owing to its superior piezoelectric properties[1]. However, the environment pollution caused by highly toxic lead (Pb) has induced an urgent need in developing various lead-free piezoelectric ceramics for the demands of various applications.[2–4] Therefore, much effort has been made to improve the properties of conventional lead-free piezoelectric ceramics, such as bismuth sodium titanate (BNT) and potassium sodium niobate (KNN) that could be comparable with the PZT family.[5–8] Nevertheless, their piezoelectric properties is still too low (d_{33} = 100–200 pC/N) compared with PZT. Through the combination of a morphotropic phase boundary (MPB) and processing of highly textured polycrystals, the piezoelectric constant d_{33} can be close to 400 pC/N,[2] but it is still half of that of high-end PZT.

The newly discovered lead-free BCTZ ceramics by Liu and Ren[9] have attracted great attention[10–15] due to the excellent piezoelectric properties (with d_{33} = 500–600 pC/N). The highest d_{33} of these literatures is only 350 pC/N, which is far inferior to that of Liu's report. The gap between Liu's and the others' is so big that doubt might arise. Although four elements relationship of composition–structure–properties–processing in materials science has been the core of material for a long time, unfortunately, most of the subsequent literatures seemed to pay much more attention to the compositions such as Ba/Ca or Ti/Zr ratio, and did not care so much about the processing. The ceramics with the same composition fabricated with different processes, even if the same technique but different processing parameters, they can exhibit absolutely different microstructure, then their properties may differ greatly. Before investigating the effect of compositions on the piezoelectric properties, it is strongly advised the best process parameters of the conventional ceramics should be chosen, because it makes a great difference, which will be reported in this work. As for the conventional solid-state reaction process, the most important would be the calcination and sintering temperature.[16–19] Therefore, it is necessary to investigate the effect of calcination and sintering temperature on the structure and properties of BCTZ ceramics.

* Corresponding author. Tel.: +86 21 52411066; fax: +86 21 52413122.
E-mail address: yxli@mail.sic.ac.cn (Y. Li).

0955-2219/$ – see front matter © 2011 Elsevier Ltd. All rights reserved.
doi:10.1016/j.jeurceramsoc.2011.04.023

In this paper, the dielectric and piezoelectric properties of BCTZ ceramics calcined and sintered at different temperatures are studied. With the optimized processing, the highest d_{33} in BCTZ system was obtained. In addition, electromechanical coupling factor, mechanical quality factor and ferroelectric properties of BCTZ ceramics are presented.

2. Experimental procedure

2.1. Sample preparation

The $(Ba_{0.85}Ca_{0.15})(Ti_{0.9}Zr_{0.1})O_3$ (BCTZ) ceramics were prepared via conventional solid-state reaction process. The oxide or carbonate powders of $BaCO_3$ (99.0%, $d_{50} < 0.5$ μm, Sinopharm Chemical Reagent Co. China), $CaCO_3$ (99.96%, $d_{50} < 0.8$ μm, Wuxi Kaimao Chemicals Co. China), ZrO_2 (99.9%, $d_{50} < 2$ μm, Jishui Jixiang Co. China) and TiO_2 (99.84%, $d_{50} = 0.5$–0.8 μm, Xiantao Zhongxing Electronic Material Co. China) were used as raw materials. They were wet milled in a nylon jar with zirconia balls for 5 h. Then the mixed powders were dried and calcined at 1000 °C, 1100 °C, 1200 °C and 1300 °C for 2 h in air, respectively. These calcined powders were ball milled again in anhydrous ethanol for 5 h, the dried powders were mixed with 6 wt.% polyvinyl alcohol (PVA) and pressed into disks with a diameter of 15 mm by uniaxial pressing at 150 MPa. After excluding PVA binder at 800 °C for 1 h, the pressed pellets were sintered at 1500–1550 °C for 2 h in air.

2.2. Characterization

For measuring electrical properties, silver paste was coated on both polished surfaces of the sintered samples and fired at 700 °C for 30 min to form Ag electrodes. Specimens for piezoelectric measurements were polarized at room temperature in a silicone oil bath by applying a dc electric field of 3 kV/mm for 20 min. Piezoelectric properties were measured after laying the polarized specimens for 24 h to release the remnant stress and charge.

The calcined powders and sintered samples were characterized by XRD patterns using a Cu-K_α radiation ($\lambda = 1.54178$ Å). Volume density (ρ_v) and relative density (ρ_r) of the sintered specimens were measured by Archimedes method using deionized water as medium. The microstructure of the ceramics was studied by electron probe microanalysis (EPMA, 8705QH2, Shimadzu, Tokyo, Japan) after polished and thermally etched at 1400 °C for 10 min. Piezoelectric coefficient d_{33} values were measured by a quasi-static d_{33} meter (ZJ-3A, Institute of Acoustics, Chinese Academy of Sciences, Beijing, China). Electromechanical coupling factor of thickness (k_t), planar (k_p) and transverse (k_{31}), mechanical quality factor (Q_m), piezoelectric constant d_{31} and elastic compliance constants s_{11}^E of the poled samples were measured by resonance–antiresonance method with an impedance analyzer (Wayne Kerr 6500B, UK). Temperature dependence of dielectric constant (ε_r) and dielectric loss ($\tan\delta$) of the poled samples at 10^3–10^6 Hz was measured with a multifrequency LCR meter (Hewlett Packard, HP4192A, USA). Ferroelectric hysteresis loops (P–E) were measured by a modified Sawyer-Tower circuit at 10 Hz at different temperatures (TF Analyzer 2000, aixACCT Systems GmbH, Aachen, Germany).

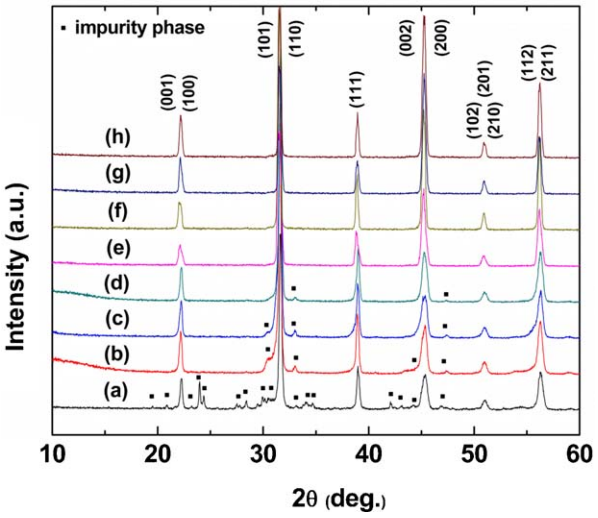

Fig. 1. X-ray diffraction patterns of $(Ba_{0.85}Ca_{0.15})(Ti_{0.9}Zr_{0.1})O_3$: (a) powders, $T_{cal} = 1000$ °C; (b) powders, $T_{cal} = 1100$ °C; (c) powders, $T_{cal} = 1200$ °C; (d) powders, $T_{cal} = 1300$ °C; (e) ceramics, $T_{cal} = 1000$ °C, $T_s = 1520$ °C; (f) ceramics, $T_{cal} = 1100$ °C, $T_s = 1520$°C; (g) ceramics, $T_{cal} = 1200$ °C, $T_s = 1520$ °C; (h) ceramics, $T_{cal} = 1300$ °C, $T_s = 1520$ °C.

3. Results and discussion

3.1. XRD characterization of calcined powders and sintered ceramics

The XRD patterns of the powders and ceramics calcined and sintered at different temperatures are illustrated in Fig. 1. The raw material powders calcined at 1000 °C, 1100 °C, 1200 °C and 1300 °C, respectively, for 2 h did not form pure perovskite phase. It can be seen that the sorts and amount of impurity phases decrease with increased calcination temperature (T_{cal}), and there is only a trace of impurity in the powders calcined at 1300 °C. Nevertheless, all the ceramics sintered at 1520 °C formed pure perovskite phase, implying that different T_{cal} do not lead to obvious change in the phase structure of the ceramics, i.e. the impurity phase will diffuse into BCTZ lattices to form a solid solution finally. Accordingly, the ceramics sintered at higher temperatures will also form pure perovskite phase.

3.2. Density and microstructure

Fig. 2 shows the effect of sintering temperature (T_s) on the volume densities (ρ_v) and relative densities (ρ_r) of BCTZ ceramics calcined at different temperatures. As the ceramics sintered at different temperatures all formed MPB between tetragonal and rhombohedral phases at room temperature,[9] it is not easy to determine the accurate value of the theoretical density (ρ_t), and no relative or theoretic density is reported for MPB composition ceramics. However, since the distortion between the tetragonal and rhombohedral phase is tiny, herein, we substitute the ρ_t (5.687 g/cm^3 with $a = 4.0149$ Å, $c = 4.0394$ Å) of tetragonal phase calculated from XRD results for that of BCTZ ceramics,

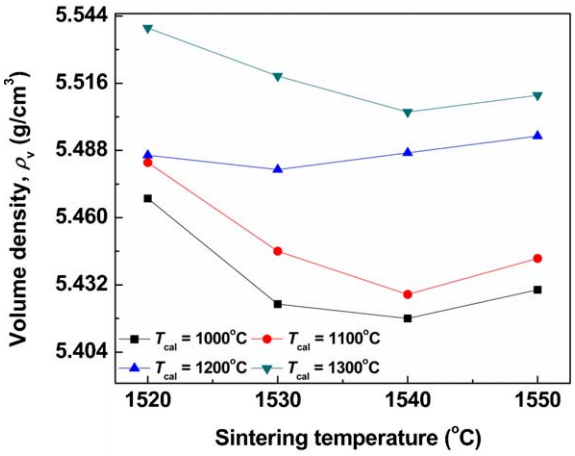

Fig. 2. Effect of sintering temperature on the volume density of BCTZ ceramics calcined at different temperatures.

which provides a very close value for comparison study. With this approximation, we can see that ρ_r of all the ceramics exceeds 95%. The density increases significantly as the T_{cal} increases, while the density first decreases as T_s increases to 1540 °C, and then increases slightly as T_s further increases. We can see that T_{cal} has a greater influence on the density of ceramics than T_s. So the increasing calcination temperature is beneficial to obtain dense BCTZ ceramics.

Fig. 3 shows the EPMA micrographs of polished surfaces of BCTZ ceramics calcined and sintered at various temperatures. It can be seen from Fig. 3(a)–(d) that T_{cal} has varying influences on the pore size and distribution, grain size, and grain boundary. As the T_{cal} increases, the pore size tends to increase, but there seems to be less pores with higher T_{cal}. The influence of T_{cal} on grain size is shown in Fig. 4(a). The grain size increases a little with T_{cal}. The influence of T_{cal} on grain boundary should be emphasized here. As T_{cal} increases, the grain boundaries become blurred. All the polished samples were thermally etched at the same condition (1400 °C for 10 min), however, the grain boundary is more difficult to be etched for higher temperature calcined ceramics. For the sample with T_{cal} = 1000 °C, the grain boundaries are etched into grooves and they can be easily recognized. While as the T_{cal} increases, the grain boundary could hardly be etched at 1400 °C for 10 min. Then, the grain boundaries appeared blurred and narrowed as T_{cal} increases. Because the atoms at grain boundary can diffuse into the adjacent grains when sintered at high temperature, and with higher T_{cal} this diffusion becomes much easier due to the shorter diffusion distances between grains.

From Fig. 3(c and e–h) it can be seen that the T_s has an influence on the grain size and pore size, but almost no influence on the grain boundary. The average grain size as a function of T_s is shown in Fig. 4(b). As the T_s increases, the grain size increases obviously. It can be concluded that the grain size is mainly controlled by T_s, while the grain boundary is dominated by T_{cal}. These two parameters of solid-state reaction process have an important influence on the microstructure of the BCTZ ceramics, and hence influence the electrical properties of the ceramics.

3.3. Piezoelectric properties, electromechanical coupling factor and mechanical quality factor

Fig. 5 shows the effect of T_s on the d_{33} of BCTZ ceramics calcined at different temperatures. On the one hand, for the ceramics sintered at the same temperature, d_{33} increases steadily as the T_{cal} increases. Furthermore, the effect of T_s on d_{33} becomes more obvious as T_{cal} increases. This result indicates the grain boundary basically controlled by T_{cal} could greatly affect the piezoelectric properties. Because the atomic arrangement at the "blurred" grain boundaries is much more similar to that in the grains, resulting a decrease in internal stress, which will induce continuity of strain in the grain boundaries and result in continuity of domains across the grain boundaries.[20] While the atomic arrangement at the grain boundaries of the ceramics with low T_{cal} is relatively irregular and domains across the grain boundaries are not continuous. The continuity of domains across the grain boundaries is beneficial to the piezoelectric properties, and then the d_{33} of the ceramics with "blurred boundaries" is much higher. However, further work to clarify the domain configuration and microstructure of blurred grain boundaries using HRTEM is needed.

On the other hand, for the ceramics calcined at the same temperatures, the d_{33} increases to the maximum value as T_s increases to 1540 °C and then decreases as T_s further increases. Both density and grain size have an important effect on the piezoelectric constant.[21] The ceramics sintered at 1540 °C do not have the maximum density but have the largest d_{33}, that is because grain size affects d_{33} more markedly than density.[22] In order to get good piezoelectric properties, T_s must be optimized to obtain an appropriate grain size.

Large grain size is another characteristic of the BCTZ ceramics sintered at such a high temperature.[13,15] The grain size is much larger than 10 μm, while the grain size of other lead-free piezoelectric ceramic systems such as BNT and KNN systems is only 3 μm.[23,24] That is because the sintering temperature is high enough for the grain growth of the BCTZ systems, while for BNT or KNN system, the sintering temperature is usually just adequate for densification due to the volatilization of Bi_2O_3, K_2O and Na_2O at higher temperature. Generally speaking, the calcined powders with the same composition of ceramics are used as supporting powders for ceramic pellets when being sintered. These powders begin to melt when the temperature rises to 1450 °C, limiting T_s not high enough for grain growth.[10,12,13,15] Here, ZrO_2 powders were used to support the pellets and the T_s can be elevated to as high as 1550 °C. A maximum value of d_{33} = 650 pC/N was obtained at T_{cal} = 1300 °C and T_s = 1540 °C.

Fig. 6 shows the effect of T_s on k_p, k_t and Q_m of BCTZ ceramics calcined at different temperatures. Both k_p and k_t increase significantly as T_{cal} increases. The value of k_p increases firstly and then decreases with increasing T_s, while k_t increases monotonously as T_s increases. The maximum k_p was obtained at T_s = 1540 °C. The maximum k_p and k_t were 0.53 (T_{cal} = 1300 °C, T_s = 1540 °C) and 0.44 (T_{cal} = 1300 °C, T_s = 1550 °C), respectively. However, the variation of Q_m with T_{cal} and T_s was opposite to those of d_{33}, k_p and k_t. Q_m decreases as T_{cal} and

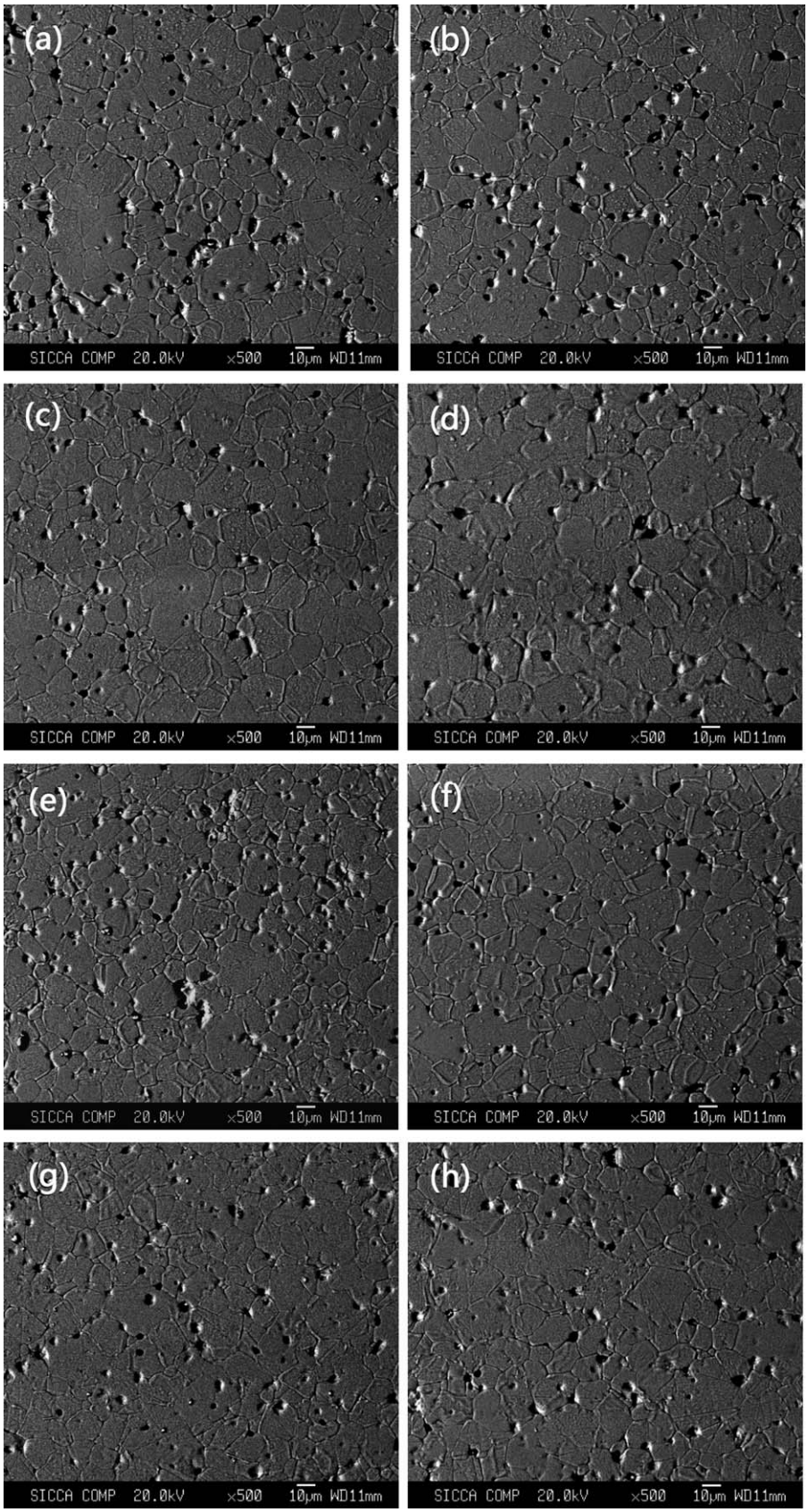

Fig. 3. EPMA micrographs of polished surfaces for BCTZ ceramics calcined and sintered at various temperatures: (a) $T_{cal} = 1000\,^{\circ}C$, $T_s = 1540\,^{\circ}C$; (b) $T_{cal} = 1100\,^{\circ}C$, $T_s = 1540\,^{\circ}C$; (c) $T_{cal} = 1200\,^{\circ}C$, $T_s = 1540\,^{\circ}C$; (d) $T_{cal} = 1300\,^{\circ}C$, $T_s = 1540\,^{\circ}C$; (e) $T_{cal} = 1200\,^{\circ}C$, $T_s = 1500\,^{\circ}C$; (f) $T_{cal} = 1200\,^{\circ}C$, $T_s = 1520\,^{\circ}C$; (g) $T_{cal} = 1200\,^{\circ}C$, $T_s = 1530\,^{\circ}C$; (h) $T_{cal} = 1200\,^{\circ}C$, $T_s = 1550\,^{\circ}C$.

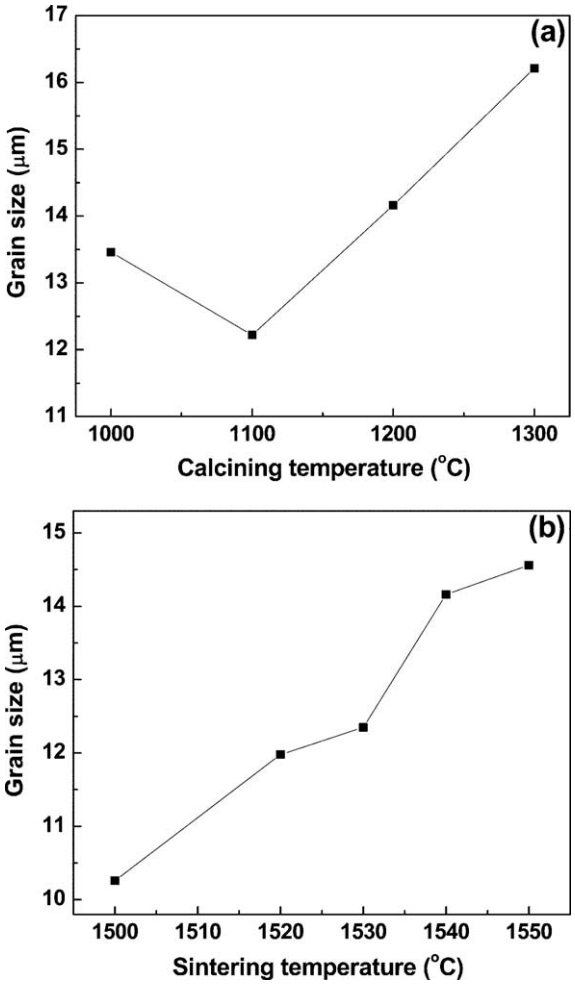

Fig. 4. Average grain size of BCTZ ceramics (a) sintered at 1540 °C and calcined at different temperatures and (b) calcined at 1200 °C and sintered at different temperatures.

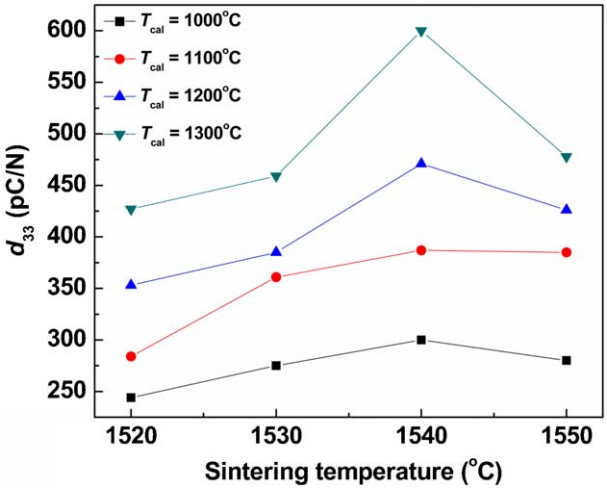

Fig. 5. Effect of sintering temperature on the d_{33} of BCTZ ceramics calcined at different temperatures.

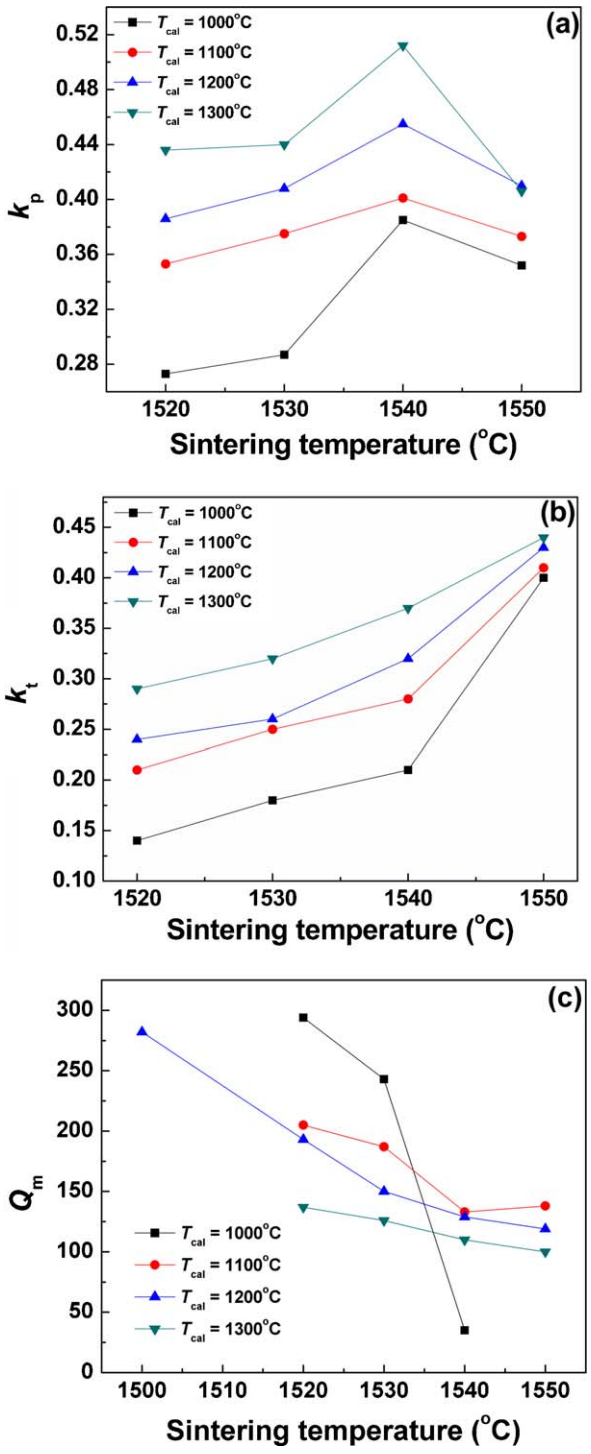

Fig. 6. Effect of sintering temperature on the (a) k_p, (b) k_t and (c) Q_m of BCTZ ceramics calcined at different temperatures.

T_s increase, it tends to have a smaller value when d_{33}, k_p and k_t get a larger value. This result is similar to Ref. 25.

The effect of T_s on d_{31}, s_{11}^E and k_{31} of BCTZ ceramics calcined at 1300 °C is shown in Fig. 7. It can be seen that as T_s increases, d_{31}, s_{11}^E and k_{31} all increase to the maximum values at $T_s = 1540$ °C, and the maximum values are 74 pC/N, 14.0×10^{-12} m^2/N and 0.309, respectively. While d_{31}, s_{11}^E and k_{31} of the ceramics calcined at 1000 °C and sintered at 1520 °C

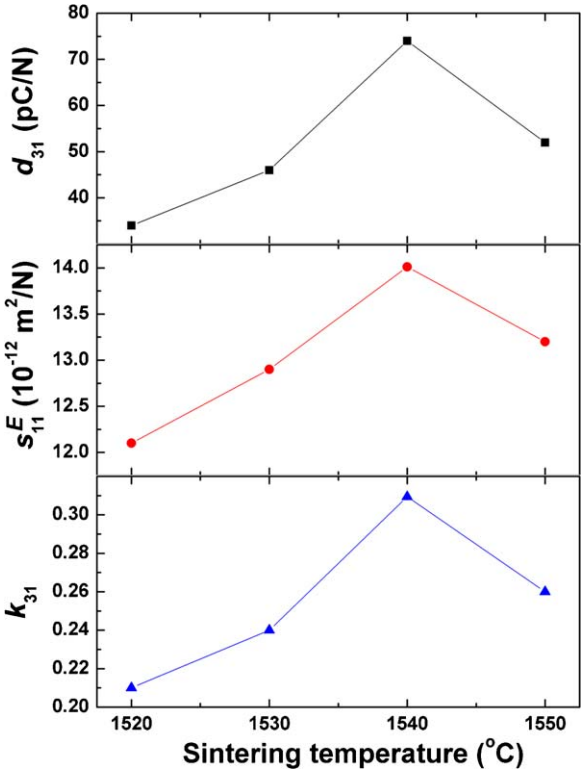

Fig. 7. Effect of sintering temperature on d_{31}, s_{11}^E and k_{31} of BCTZ ceramics calcined at 1300 °C.

are 24 pC/N, 11.97 × 10^{-12} m^2/N and 0.140, respectively, which is much lower than those calcined at 1300 °C and sintered at 1540 °C.

3.4. Dielectric properties

Fig. 8 illustrates the effect of sintering temperature on (a) dielectric constant (ε_r) and (b) dielectric loss (tan δ) of BCTZ ceramics calcined at different temperatures. We can see that with increasing T_{cal}, ε_r increases obviously. While as T_s increases, ε_r first increases to its maximum value at $T_s = 1540$ °C and then decreases. At $T_{cal} = 1300$ °C and $T_s = 1540$ °C, $\varepsilon_r = 4500$. This phenomenon is in accordance with piezoelectric constant results in Fig. 5. While tan δ increases as T_s and T_{cal} increase. The increase in tan δ might be ascribed to the presence of oxygen vacancy generated at higher temperature.

Fig. 9 exhibits the temperature dependence of dielectric constant and dielectric loss of BCTZ ceramics calcined at 1300 °C and sintered at 1540 °C at different frequency. As it can be seen, two peaks are observed on the dielectric constant versus temperature curves ($\varepsilon_r - T$) in the measured temperature range between 15 °C and 200 °C. The first peak corresponds to polymorphic phase transitions from rhombohedral phase to tetragonal phase (T_{r-t}) at 32°C. The second peak corresponds to transitions from tetragonal phase to cubic phase (T_c) at 85 °C, which is lower than Ref. 9, but much larger than Ref. 13. There are also two peaks on the dielectric loss versus temperature curves (tan $\delta - T$), which is similar to the curves of $\varepsilon_r - T$. However, the temperatures of the peaks of tan $\delta - T$ is lower than that of $\varepsilon_r - T$.

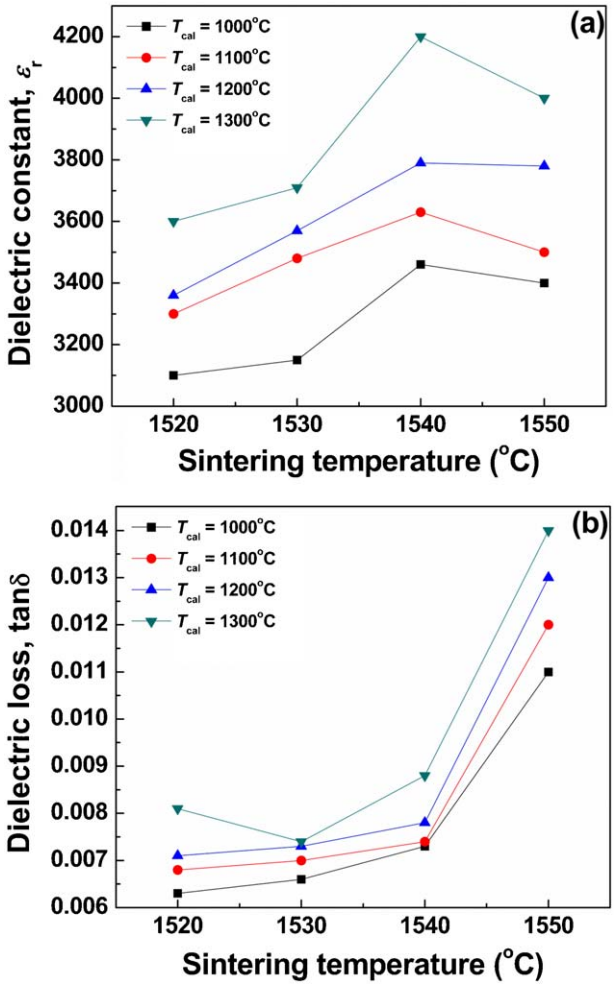

Fig. 8. Effect of sintering temperature on the (a) dielectric constant, (b) dielectric loss of BCTZ ceramics calcined at different temperatures.

3.5. Ferroelectric properties

Fig. 10(a) shows the ferroelectric properties of BCTZ ceramics sintered at 1540 °C with different calcination temperatures, which is measured at 25 °C. The ferroelectric hysteresis loops

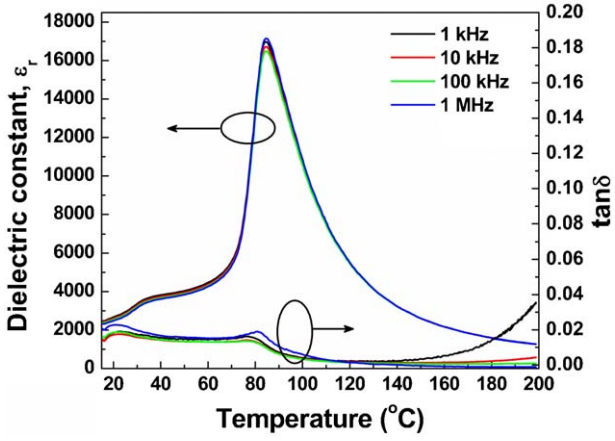

Fig. 9. Temperature dependence of dielectric constant and dielectric loss of BCTZ ceramics calcined at 1300 °C and sintered at 1540 °C.

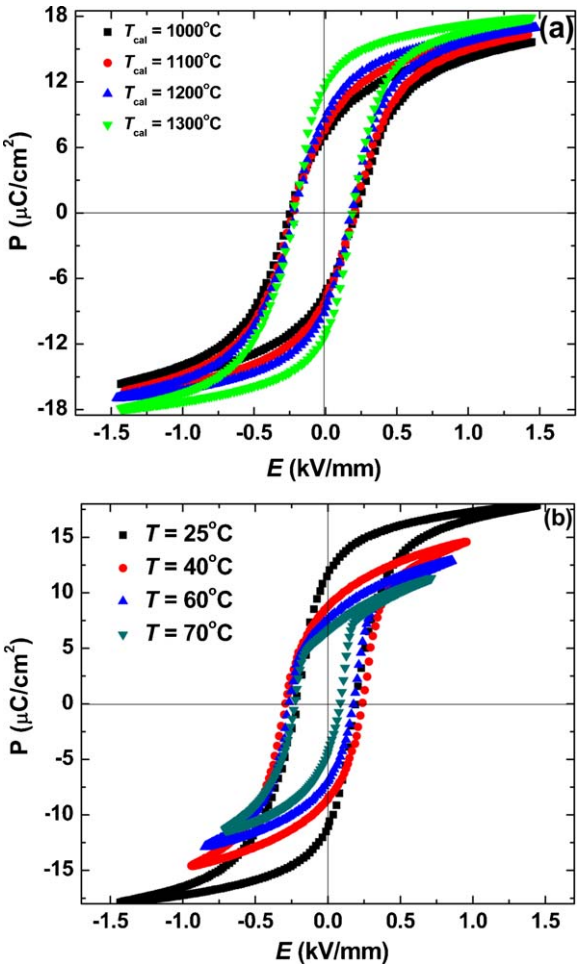

Fig. 10. (a) Effect of calcination temperature on the *P–E* hysteresis loops of BCTZ ceramics sintered at 1540 °C and measured at 25 °C; (b) temperature dependence of *P–E* hysteresis loops of BCTZ ceramics calcined at 1300 °C and sintered at 1540 °C.

with a good square shape for all the ceramics are clearly observed in Fig. 10(a). Remnant polarization P_r increases from 7.18 to 11.69 μC/cm^2 as the T_{cal} increases from 1000 °C to 1300 °C, which is much higher than previously reported $(Ba_{1-x}Ca_x)(Ti_{0.9}Zr_{0.1})O_3$ ceramics.[13] As the T_{cal} increases, the coercive field E_c first decreases to 182 V/mm at T_{cal} = 1200 °C and then increases slightly to 190 V/mm, which is a little higher than Ref. 9. Fig. 10(b) illustrates the *P–E* loops of ceramics (T_{cal} = 1300 °C, T_s = 1540 °C) measured at different temperatures. P_r decreases from 11.69 μC/cm^2 to 6.55 μC/cm^2 as the measured temperature increases from 25 °C to 70 °C.

4. Conclusions

The electrical properties of $(Ba_{0.85}Ca_{0.15})(Ti_{0.9}Zr_{0.1})O_3$ lead-free piezoceramics prepared at different calcination temperatures from 1000 °C to 1300 °C, and at different sintering temperatures from 1520 °C to 1550 °C were investigated. The X-ray diffraction analysis showed that T_{cal} has a significant influence on the phase structure of the calcined powders, but there is almost no influence on the phase structure of final sintered ceramics. T_{cal} has a significant influence on density and grain boundary, while T_s has an obvious influence on grain size. With optimized T_{cal} and T_s, we can obtain desired microstructure, which is beneficial to piezoelectric properties of the ceramics. The BCTZ ceramics calcined at 1300 °C and sintered at 1540 °C exhibit excellent properties of d_{33} = 650 pC/N, d_{31} = 74 pC/N, k_p = 0.53, k_t = 0.38, k_{31} = 0.309, $s_{11}^E = 14.0 \times 10^{-12} m^2/N$, ε_r = 4500, tan δ = 0.009, T_c = 85 °C, P_r = 11.69 μC/cm^2 and E_c = 190 V/mm. The present study demonstrates that the calcination and sintering temperatures play a very important role in the microstructure, dielectric and piezoelectric properties of BCTZ ceramics, which is important to guide the design of BCTZ-based lead-free ceramics with enhanced piezoelectric properties.

Acknowledgements

This work was supported by the Ministry of Sciences and Technology of China through 973-Project (2009CB613305), The Major Program of the National Natural Science Foundation of China (50932007), and The Science & Technology Commission of Shanghai Municipality (10XD1404700).

References

1. Tressler JF, Alkoy S, Newnham RE. Piezoelectric sensors and sensor materials. *Journal of Electroceramics* 1998;**2**(4):257–72.
2. Saito Y, Takao H, Tani T, Nonoyama T, Takatori K, Homma T, Nagaya T, Nakamura M. Lead-free piezoceramics. *Nature* 2004;**432**(7013):84–7.
3. Cross E. Materials science: lead-free at last. *Nature* 2004;**432**(7013):24–5.
4. Damjanovic D. Materials for high temperature piezoelectric transducers. *Current Opinion in Solid State and Materials Science* 1998;**3**(5):469–73.
5. Du H, Tang F, Luo F, Zhu D, Qu S, Pei Z, Zhou W. Influence of sintering temperature on piezoelectric properties of $(K_{0.5}Na_{0.5})NbO_3$–$LiNbO_3$ lead-free piezoelectric ceramics. *Materials Research Bulletin* 2007;**42**(9):1594–601.
6. Li JF, Wang K, Zhang BP, Zhang LM. Ferroelectric and piezoelectric properties of fine-grained $Na_{0.5}K_{0.5}NbO_3$ lead-free piezoelectric ceramics prepared by spark plasma sintering. *Journal of the American Ceramic Society* 2006;**89**(2):706–9.
7. Li EZ, Suzuki R, Hoshina T, Takeda H, Tsurumi T. Dielectric, piezoelectric, and electromechanical phenomena in $(K_{0.5}Na_{0.5})NbO_3$–$LiNbO_3$–$BiFeO_3$–$SrTiO_3$ ceramics. *Applied Physics Letters* 2009;**94**(13):132903.
8. Hiruma Y, Nagata H, Takenaka T. Depolarization temperature and piezoelectric properties of $(Bi_{1/2}Na_{1/2})TiO_3$–$(Bi_{1/2}Li_{1/2})TiO_3$–$(Bi_{1/2}K_{1/2})TiO_3$ lead-free piezoelectric ceramics. *Ceramics International* 2009;**35**(1):117–20.
9. Liu WF, Ren XB. Large piezoelectric effect in Pb-free ceramics. *Physical Review Letters* 2009;**103**(25):257602.
10. Li W, Xu Z, Chu R, Fu P, Zang G. Piezoelectric and dielectric properties of $(Ba_{1-x}Ca_x)(Ti_{0.95}Zr_{0.05})O_3$ lead-free ceramics. *Journal of the American Ceramic Society* 2010;**93**(10):2942–4.
11. Porta M, Lookman T, Saxena A. Effects of criticality and disorder on piezoelectric properties of ferroelectrics. *Journal of Physics: Condensed Matter* 2010;**22**(34):345902.
12. Li W, Xu Z, Chu R, Fu P, Zang G. High piezoelectric d_{33} coefficient in $(Ba_{1-x}Ca_x)(Ti_{0.98}Zr_{0.02})O_3$ lead-free ceramics with relative high Curie temperature. *Materials Letters* 2010;**64**(21):2325–7.
13. Li W, Xu Z, Chu R, Fu P, Zang G. Polymorphic phase transition and piezoelectric properties of $(Ba_{1-x}Ca_x)(Ti_{0.9}Zr_{0.1})O_3$ lead-free ceramics. *Physica B: Condensed Matter* 2010;**405**(21):4513–6.

14. Damjanovic D. A morphotropic phase boundary system based on polarization rotation and polarization extension. *Applied Physics Letters* 2010;**97**(6):062906.
15. Zhang SW, Zhang HL, Zhang BP, Yang S. Phase-transition behavior and piezoelectric properties of lead-free $(Ba_{0.95}Ca_{0.05})(Ti_{1-x}Zr_x)O_3$ ceramics. *Journal of Alloys and Compounds* 2010;**506**(1):131–5.
16. Jiang MH, Liu XY, Cheng J, Zhou XJ, Deng MJ. Effects of sintering temperature on the microstructure and electrical properties of $BiMnO_3$-doped $0.95Na_{0.5}K_{0.5}NbO_3$–$0.05LiSbO_3$ ceramics. *Materials and Manufacturing Process* 2010;**25**(8):730–4.
17. Wu JM, Chang MC, Yao PC. Reaction sequence and effects of calcination and sintering on microwave properties of (Ba,Sr)O–Sm_2O_3–TiO_2 ceramics. *Journal of the American Ceramic Society* 1990;**73**(6): 1599–605.
18. Pokharel BP, Datta MK, Pandey D. Influence of calcination and sintering temperatures on the structure of $(Pb_{1-x}Ba_x)ZrO_3$. *Journal of Materials Science* 1999;**34**(4):691–700.
19. Zhen Y, Li JF. Normal sintering of (K,Na)NbO_3-based ceramics: influence of sintering temperature on densification, microstructure, and electrical properties. *Journal of the American Ceramic Society* 2006;**89**(12):3669–75.
20. Takahashi H, Numamoto Y, Tani J, Tsurekawa S. Considerations for $BaTiO_3$ ceramics with high piezoelectric properties fabricated by microwave sintering method. *Japanese Journal of Applied Physics* 2008;**47**(11):8468–71.
21. Zhu M, Liu L, Hou Y, Wang H, Yan H. Microstructure and electrical properties of MnO-doped $(Na_{0.5}Bi_{0.5})_{0.92}Ba_{0.08}TiO_3$ lead-free piezoceramics. *Journal of the American Ceramic Society* 2007;**90**(1):120–4.
22. Yang A, Wang CA, Guo R, Huang Y, Nan CW. Effects of sintering behavior on microstructure and piezoelectric properties of porous PZT ceramics. *Ceramics International* 2010;**36**(2):549–54.
23. Zuo R, Su S, Wu Y, Fu J, Wang M, Li L. Influence of A-site nonstoichiometry on sintering, microstructure and electrical properties of $(Bi_{0.5}Na_{0.5})TiO_3$ ceramics. *Materials Chemistry and Physics* 2008;**110**(2–3):311–5.
24. Rubio-Marcos F, Marchet P, Merle-Méjean T, Fernandez JF. Role of sintering time, crystalline phases and symmetry in the piezoelectric properties of lead-free KNN-modified ceramics. *Materials Chemistry and Physics* 2010;**123**(1):91–7.
25. Hao J, Chu R, Xu Z, Zang G, Li G. Structure and electrical properties of (Li, Sr, Sb)-modified $K_{0.5}Na_{0.5}NbO_3$ lead-free piezoelectric ceramics. *Journal of Alloys and Compounds* 2009;**479**(1–2):376–80.